Enhanced near-infrared electrochromism in triphenylamine-based aramids bearing phenothiazine redox centers†

Hung-Ju Yen and Guey-Sheng Liou*

Received 14th June 2010, Accepted 27th July 2010
DOI: 10.1039/c0jm01889a

A series of organosoluble polyamides based on *N*-phenothiazinylphenyl redox units showing anodically electrochromic characteristics both in the near-infrared (NIR) and visible light regions were prepared from the phosphorylation polyamidation reactions of a newly synthesized diamine monomer, 4,4′-diamino-4″-*N*-phenothiazinyltriphenylamine, with various dicarboxylic acids. These polymers were readily soluble in many polar solvents and showed useful levels of thermal stability associated with relatively high glass-transition temperatures (T_g) (255–277 °C) and high char yields (higher than 67% at 800 °C in nitrogen). In addition, the polymer films showed reversible electrochemical oxidation with enhanced NIR contrast, high coloration efficiency (CE), low switching time, and anodic green/purple electrochromic behaviors.

Introduction

Electrochromic materials reveal reversible optical changes in absorption or transmittance upon electrochemically oxidized or reduced, such as transition-metal oxides, inorganic coordination complexes, conjugated polymers, and organic molecules.[1] Initially, investigation of electrochromic materials directed towards optical changes in the visible region (*e.g.*, 400–800 nm), proved useful and variable applications such as *E*-paper, optical switching devices, smart window, and camouflage materials.[2] Increasingly, attention of the optical changes has been focused on extending from the near infrared (NIR; *e.g.*, 800–2000 nm) through to the microwave regions of the spectrum, which could be exploitable for optical communication, data storage, and thermal control (heat gain or loss) in buildings and spacecraft.[3] Therefore, NIR electrochromic materials including transition metal oxides (WO_3), organic metal complex (ruthenium dendrimer), and quinone-containing organic materials have been investigated in recent years.[4] Wang and Wan made efforts on the quinone-containing electrochromic materials, which revealed high absorption in the NIR upon electrochemical reduction.[4c–4g] Reynolds' group reported color-to-transmissive NIR electrochromic conjugated polymers and their device, exhibited multicolors in the neutral state and transmissive in the oxidized state.[5a] In addition to conjugated polymers,[5] the phenothiazine-containing molecule is an interesting anodic electrochromic system for NIR applications due to its particular structure and electron transfer in the oxidized states.

Phenothiazine (10*H*-dibenzo-[*b*,*e*]-1,4-thiazine; PSN) is a well-known heterocyclic compound with electron-rich sulfur and nitrogen heteroatoms. Organic molecules[6] and polymers[7] containing phenothiazine reversible redox units have recently attracted much research interest because of their unique electro-optical properties and resulting potential in diverse applications such as light-emitting diodes,[6a,7b,7c] photovoltaic devices,[6c,7d] and chemiluminescence.[7a] Interestingly, the intermolecular/intramolecular electron transfer between bridged PSN centers in the mixed-valence cation radicals state leading to the absorption bands in the NIR region, was delineated by Kochi.[8] Moreover, the absorbance of its dications also appeared in the NIR (800–1200 nm) range due to the nearly coplanar structure of PSN redox centers ($\theta = 172°$), indicating a great potential in anodic electrochromic systems for NIR applications.

Triarylamine derivatives are well known as its photo- and electroactive properties have potential for optoelectronic applications, such as photoconductors, hole-transporters, light-emitters, and memory devices.[9] Electron-rich triarylamines can be easily oxidized to form stable radical cations, and the oxidation process is always associated with a noticeable change of coloration. Thus, studies of the synthesis and electrochromism of triarylamine-based polymers have been reported in the literature.[10] Since 2005, our groups have initiated some high-performance polymers (*e.g.*, aromatic polyamides and polyimides) bearing the triarylamine unit as an electrochromic functional moiety.[11] It has also been reported in our previous publications[12] that the incorporation of electron-donating substituents such as methoxy and *tert*-butyl groups at the *para*-position of phenyl groups on the electrochemically active sites of the triphenylamine (TPA) unit resulted in stable TPA cationic radicals and decreased oxidation potential, leading to a significantly enhanced redox and electrochromic stability of the prepared polyamides.

In this article, we therefore synthesized the novel PSN-TPA-based monomer, 4,4′-diamino-4″-*N*-phenothiazinyltriphenylamine (**4**), and its derived polyamides containing electroactive

Functional Polymeric Materials Laboratory, Institute of Polymer Science and Engineering, National Taiwan University, 1 Roosevelt Road, 4th Sec., Taipei, 10617, Taiwan. E-mail: gsliou@ntu.edu.tw

† Electronic supplementary information (ESI) available: Detailed experiments and characterizations of monomers were described. Inherent viscosity, molecular weights, solubility behavior, and thermal properties of polyamides, and electrochemical properties of model compounds are provided in Tables. Figures showing NMR spectra of **3**, **4**, and **Ib**. IR, TGA, TMA curves, UV-visible transmission spectra, electrochemical properties of polyamides, and electrochemical properties of model compounds are provided. See DOI: 10.1039/c0jm01889a

TPA groups with *para*-substituted phenothiazinyl moieties which could not only greatly prevent the electrochemical coupling reactions by affording stable cationic radicals but also enhance the NIR absorption during oxidative procedure. It is well known that the aromatic polyamides as microelectronic materials have attracted great interest due to their outstanding thermal and mechanical resistance.[13] Incorporation of packing-disruptive TPA and PSN units into polyamides not only preserves high thermal stability, glass transition temperature, and solubility for enhancing film-forming ability which is beneficial for their fabrication of large-area, thin-film electrochromic devices but also provides the electroactive center to facilitate both processing and electrochromic applications. We anticipated that the prepared polyamides should be stable for multiple electrochromic switching, improving optical response times, and enhancing CE with high NIR contrast. For a comparative study, electrochemical and electrochromic properties of the present polyamides were also compared with that of structurally related ones from *N*,*N*-bis(4-aminophenyl)-*N*′,*N*′-diphenyl-1,4-phenylenediamine (**4′**) that has been reported previously.[11]

Results and discussion

Monomer synthesis

N-(4-Aminophenyl)phenothiazine (**2**) was prepared by the CsF-mediated, aromatic fluoro-displacement reaction of phenothiazine with 4-fluoronitrobenzene followed by hydrazine Pd/C-catalytic reduction according to the synthetic route outlined in Scheme 1. The new aromatic diamine having a bulky pendent *N*-phenothiazine group, 4,4′-diamino-4″-*N*-phenothiazinyltriphenylamine (**4**), was successfully synthesized by hydrazine Pd/C-catalyzed reduction of the dinitro compound **3** resulting from double *N*-arylation reaction of compound **2** with 4-fluoronitrobenzene in the presence of caesium fluoride. Elemental analysis, FAB-MS, IR, and NMR spectroscopic techniques were used to identify structures of the intermediate compounds **1–3**, and the target diamine monomer **4**. Fig. S1 and S2 (ESI†) illustrate the ^{1}H NMR and ^{13}C NMR spectra of the dinitro compound **3** and diamine monomer **4**, respectively. Assignments of each carbon and proton are assisted by the two-dimensional NMR spectra shown in Fig. S3 and S4,† and these spectra agree well with the proposed molecular structure.

Polymer synthesis

According to the phosphorylation technique first described by Yamazaki,[14] a series of novel polyamides **I** with pendent *N*-phenothiazinylphenyl units were synthesized from the diamine monomer **4** with various dicarboxylic acids **5a–5d** (Scheme 2). The polymerization was carried out *via* solution polycondensation using triphenyl phosphite and pyridine as condensing agents. All polymerization reactions proceeded smoothly and gave high molecular weights. The obtained polyamides had inherent viscosities in the range of 0.29–0.36 dL/g with weight-average molecular weights (M_w) and degree of polymerization (DP) in the range of 38500–160900 daltons and 42–114, respectively, relative to polystyrene standards (Table S1†). All the polymers could afford transparent and tough films *via* solution casting, indicating high molecular weights.

The structures of polyamides were confirmed with IR and NMR spectroscopy. A typical FT-IR spectrum for polyamide **Ic** is given in Fig. S5.† The characteristic IR absorption bands of the amide group appeared at 3304 (N–H stretch) and 1654 cm^{-1} (amide carbonyl). ^{1}H NMR and ^{13}C NMR spectra of polyamide **Ib** are illustrated in Fig. S6.† Assignments of each carbon and proton are given in the figure and assisted by the

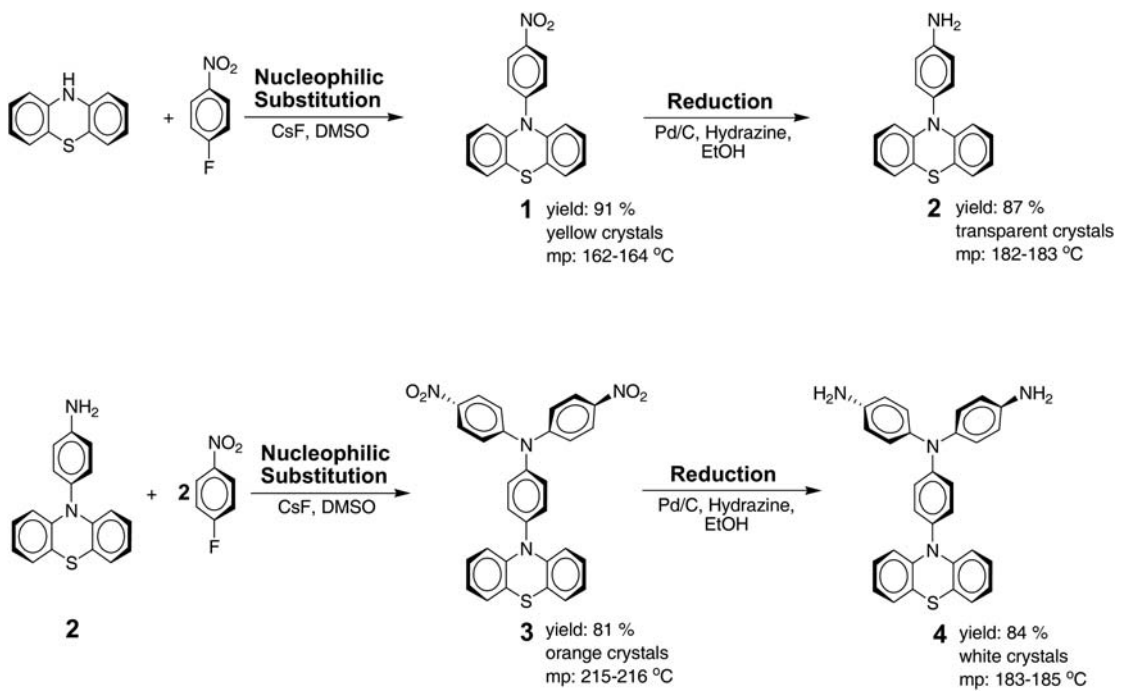

Scheme 1 Synthetic route to diamine monomer **4**.

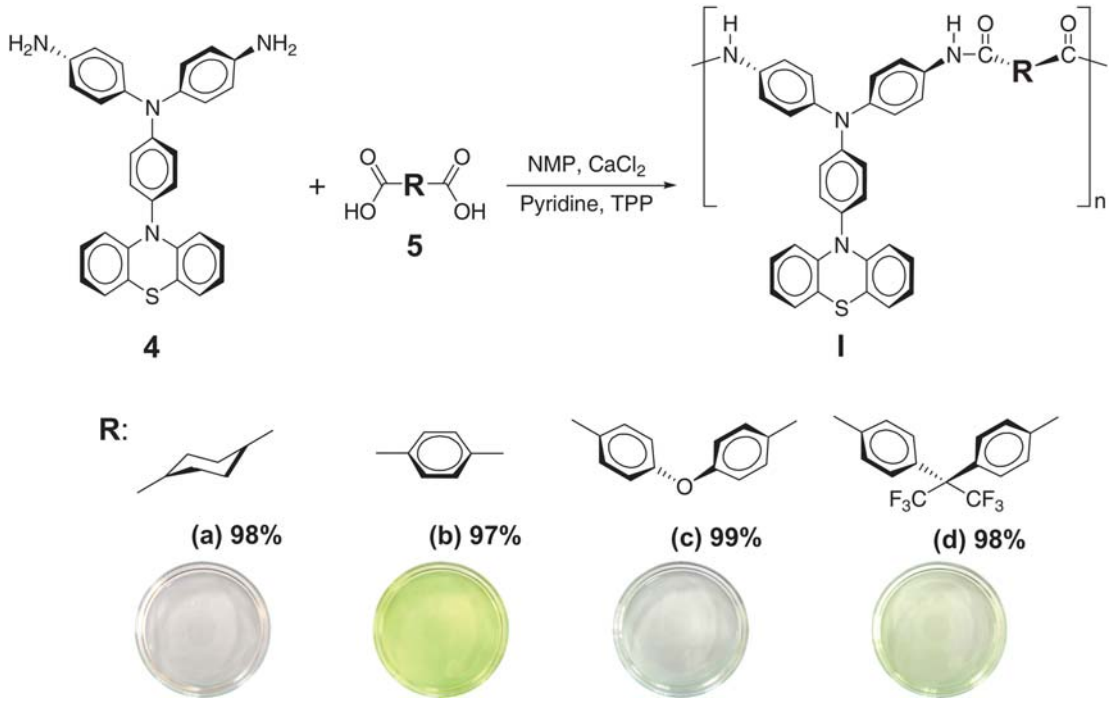

Scheme 2 Synthesis of aromatic polyamides **Ia–Id**. The photograph shows appearance of the polyamide films (thickness ~3 μm).

two-dimensional C–H HMQC NMR spectra (Fig. S7†), and these spectra agree well with the proposed polymer structure. A structurally related polyamide **I′c** derived from diamine **4′** is used for comparison studies. The synthesis and characterization of polymer **I′c** has been described previously.[11b]

Solubility and film property

The solubility behavior of aromatic–aliphatic polyamide **Ia** and aromatic polyamides **Ib–Id** was tested qualitatively, and the results are presented in Table S2.† All the polymers were readily soluble in polar aprotic organic solvent such as NMP, DMAc, DMF, and *m*-cresol. Thus, the excellent solubility makes these polymers potential candidates for practical applications by spin-coating or inkjet-printing processes to afford high performance thin films for optoelectronic devices. As shown in Scheme 2, the cast films are transparent (for **Ia**, **Ic** and **Id**) and light yellowish green (for **Ib**) in color. Their high solubility and amorphous properties can be attributed to the incorporation of a bulky pendent *N*-phenothiazinyl group to the *para*-position of TPA backbone, which results in a high steric hindrance to close packing, and thus reduces their crystallization tendency. The cutoff wavelengths (absorption edge; λ_0) from UV-vis transmittance spectra were in the range of 366–424 nm (Fig. S8†). Due to a lower capability of charge transfer, the polyamide **Ia** film showed an almost colorless and highly optical transparency with a cutoff wavelength at 366 nm.

Thermal properties

The thermal properties of polyamides were examined by TGA, TMA, and DSC, and the thermal behavior data are summarized in Table S3.† Typical TGA curves of representative polyamide **Ic** in both air and nitrogen atmospheres are shown in Fig. S9.† All the prepared polyamides exhibited good thermal stability without significant weight loss up to 400 °C in nitrogen. The 10% weight-loss temperatures (T_d[10]) of these polymers in nitrogen and air were recorded in the range of 500–585 and 485–570 °C, respectively. The carbonized residue (char yield) of these polymers in a nitrogen atmosphere was more than 67% at 800 °C. The high char yields of these polymers can be ascribed to their high aromatic content. The glass-transition temperatures (T_g) of these polymers could be easily measured in the DSC thermograms; they were observed in the range of 255–277 °C, depending upon the stiffness of the polymer chain. All the polymers indicated no clear melting endotherms up to the decomposition temperatures on the DSC thermograms, which supports the amorphous nature of these polyamides. The softening temperatures (T_s) (may be referred as apparent T_g) of the polymer film samples were determined by the TMA method with a loaded penetration probe. They were obtained from the onset temperature of the probe displacement on the TMA traces. A typical TMA thermogram for polymer **Ia** is illustrated in Fig. S10.† In most cases, the T_s values obtained by TMA are comparable to the T_g values measured by the DSC experiments.

Electrochemical properties

The redox behavior of the polyamides were investigated by cyclic voltammetry (CV) conducted for the cast film on an ITO-coated glass substrate as working electrode in anhydrous CH_3CN and DMF containing 0.1 M of TBAP as an electrolyte under nitrogen atmosphere for oxidation and reduction measurements, respectively. Fig. 1 and Fig. S11† display the typical CV of **Ic**, which undergoes two reversible oxidation and one reduction processes. During the electrochemical oxidation of the polyamide thin

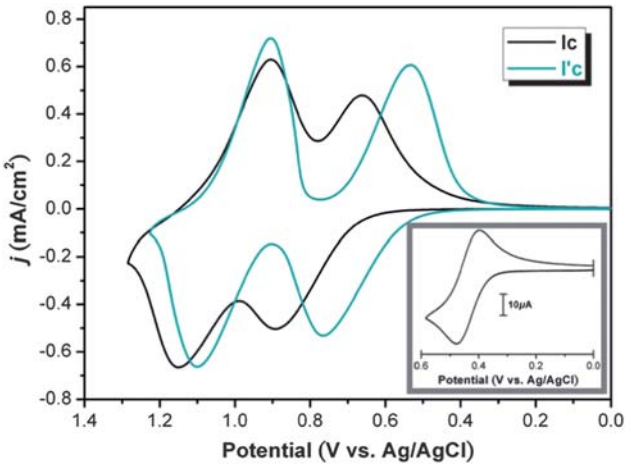

Fig. 1 Cyclic voltammograms of polyamide **Ic** and **I′c** films on an ITO-coated glass substrate and ferrocene (inset) in 0.1 M TBAP/CH_3CN at scan rate of 50 mV s^{-1}.

films, the color of the film changed from colorless to green and then to deep purple. The other polyamides showed similar CV curves to that of **Ic**. Fig. S12 and Table S4† show the electrochemical behaviour of **M1**, **M2**, and **M3**, which revealed oxidation processes at E_{onset} = 0.73, 0.75, and 0.96, respectively. Contrary to polyamide **I′c**, the first ($E_{1/2}$ = 0.75 V) and second ($E_{1/2}$ = 1.00 V) oxidation processes for polyamide **Ic** could be attributed to successive one electron removal from the phenothiazine and TPA units. Therefore, based on the CV studies of model compounds, we proposed the possible oxidative order of the nitrogen atoms for polyamide **Ic** and **I′c** in Scheme 3. The CV curve of polyamide **Ic** with higher oxidative potential was also in agreement with 1,4-bis(*N*-phenothiazinyl)benzene,[8] emphasizing the less electronic coupling interaction between *para*-phenylene-bridged redox centers than that in tetraphenyl-*p*-phenylenediamine-based polyamide **I′c**. The redox potentials of the polyamides and their respective highest occupied molecular orbital (HOMO) and lowest unoccupied molecular orbital (LUMO) (on the basis that the external ferrocene/ferrocenium redox standard is 4.8 eV below the vacuum level with E_{onset} = 0.36 V)[15] estimated from the onset of their oxidation in CV experiments are summarized in Table 1.

Spectroelectrochemistry

Spectroelectrochemical experiments were used to evaluate the optical properties of the electrochromic films. For the investigations, the polyamide film was cast on an ITO-coated glass slide, and a homemade electrochemical cell was built from a commercial ultraviolet (UV)-visible cuvette. The cell was placed in the optical path of the sample light beam in a UV-vis-NIR spectrophotometer, which allowed us to acquire electronic absorption spectra under potential control in a 0.1 M TBAP/MeCN solution. UV-vis-NIR absorbance curves correlated to applied potentials and three-dimensional transmittance-wavelength-applied potential correlation of **Ic** film were depicted in Fig. 2.

In the neutral form (0 V), the film exhibited strong absorption at around 333 nm, characteristic for triarylamine, but it was almost colorless in the visible region. Upon oxidation (increasing applied voltage from 0 to 1.05 V), the intensity of the absorption peak at 333 nm gradually decreased while a new peak at 405 nm and a broad band having its maximum absorption wavelength at

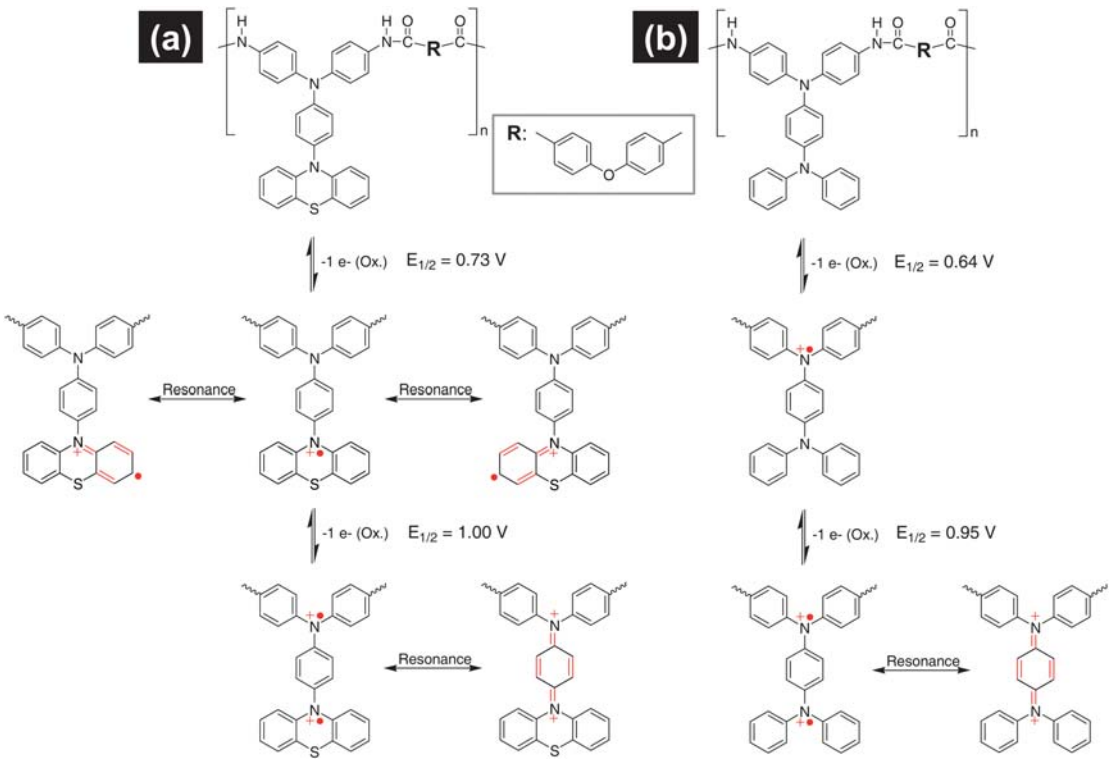

Scheme 3 The oxidation pathway of polyamide **Ic** and **I′c**.

Table 1 Redox potentials and energy levels of polyamides

	Thin films/nm		Oxidation/V[a]			Reduction/V[b]					
			$E_{1/2}$[c]								
Index	λ_{max}	λ_{onset}	1st	2nd	E_{onset}	$E_{1/2}$[c]	E_{onset}	E_g^{EC}/eV[d]	E_g^{Opt}/eV[e]	HOMO/eV[f]	LUMO/eV
Ia	326	370	0.72	0.95	0.61	−1.84	−2.00	2.61	3.35	5.05	2.44
Ib	333	426	0.73	1.00	0.61	−1.97	−2.07	2.68	2.91	5.05	2.37
Ic	333	395	0.75	1.00	0.66	−1.82	−1.94	2.60	3.16	5.10	2.50
Id	333	403	0.72	1.01	0.64	−1.92	−2.04	2.68	3.08	5.08	2.40
I′c[g]	342	393	0.64	0.95	0.54				3.16	4.98	1.82

[a] From cyclic votammograms *versus* Ag/AgCl in CH_3CN. [b] From cyclic votammograms *versus* Ag/AgCl in DMF. [c] $E_{1/2}$: Average potential of the redox couple peaks. [d] Difference between the two E_{onset} calculated from oxidation and reduction redox couples. [e] The data were calculated from polymer films by the equation: $E_g = 1240/\lambda_{onset}$ (energy gap between HOMO and LUMO). [f] The HOMO energy levels were calculated from cyclic voltammetry and were referenced to ferrocene (4.8 eV; onset = 0.36 V). [g] Data of structurally similar polyamide **I′c** having the corresponding dicarboxylic acid residue as in polyamide **Ic**.

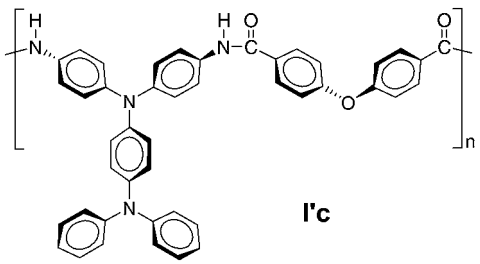

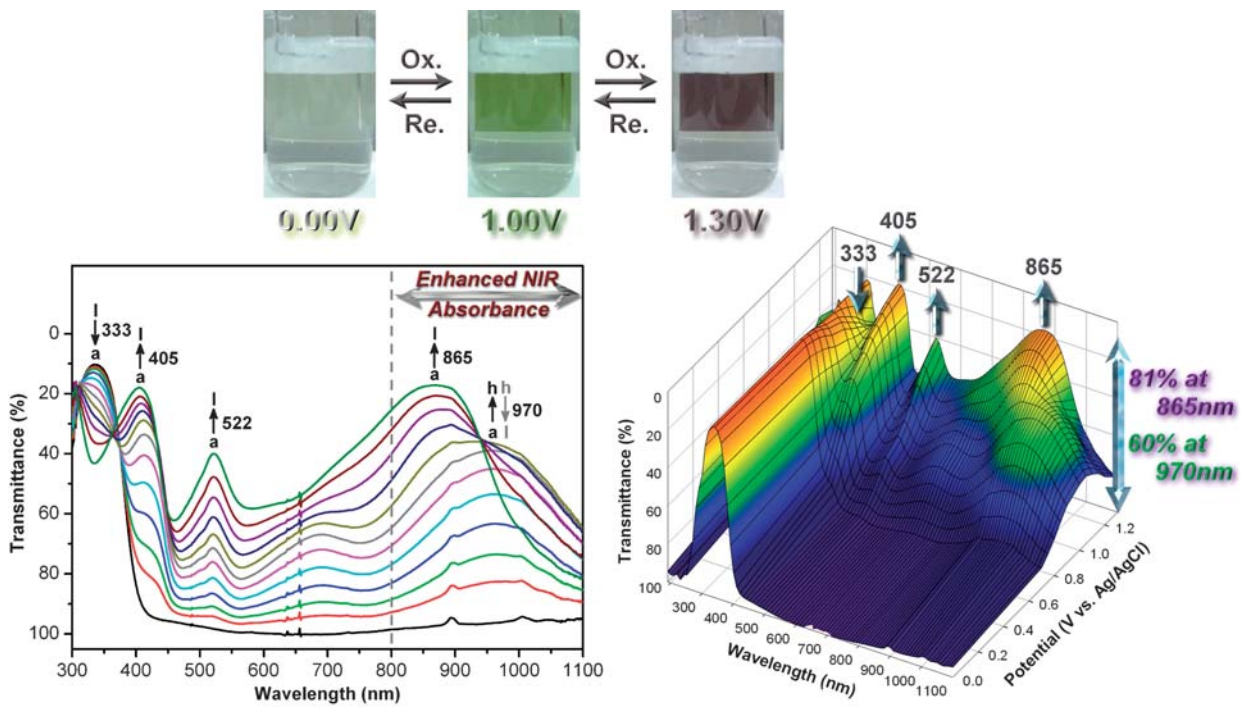

Fig. 2 Electrochromic behavior (left) at applied potentials of (a) 0.00, (b) 0.70, (c) 0.75, (d) 0.80, (e) 0.85, (f) 0.90, (g) 1.00, (h) 1.05, (i) 1.10, (j) 1.15, (k) 1.20, (l) 1.30 (V *vs.* Ag/AgCl), and 3-D spectroelectrochemical behavior (right) from 0.00 to 1.30 (V *vs.* Ag/AgCl) of polyamide **Ic** thin film (~70 nm in thickness) on the ITO-coated glass substrate in 0.1 M TBAP/CH_3CN.

970 nm in the NIR region gradually increased in intensity. We attribute the spectral change to the formation of a stable monocation radical of the PSN moiety, which was consistent with the phenomenon classified by Kochi.[8] As the more anodic potential to 1.30 V, the absorption peaks at 405 nm and 533 nm further increased with a new broad band centered at around 865 nm,

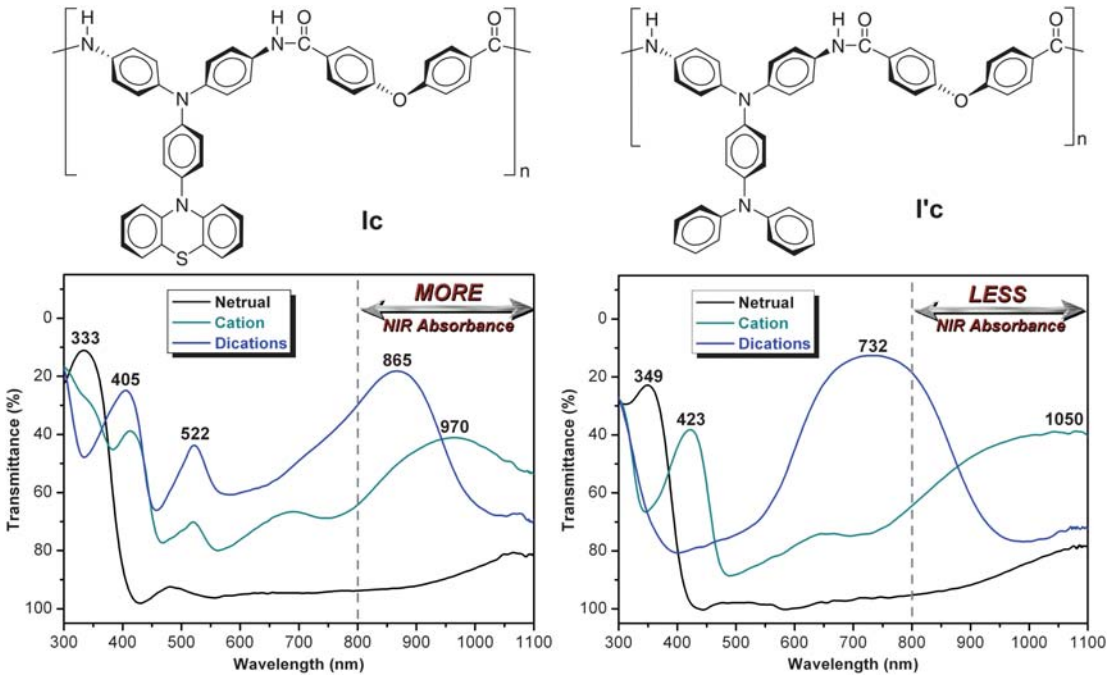

Fig. 3 Electrochromic behavior of polyamide **Ic** and **I′c** thin films on the ITO-coated glass substrate in 0.1 M TBAP/CH_3CN as their neutral, cation, and dication forms.

corresponding to the dication form. Notably, the absorption contrast in the NIR range was enhanced because of the oxidized PSN unit having a more extended conjugation length than TPA (Scheme 3), which resulted in a bathochromic shift when compared with TPA-based polyamide **I′c** as shown in Fig. 3. The observed UV-vis-NIR absorption changes in the polyamide **Ic** film at various potentials are fully reversible and are associated with strong color changes. The other polyamides showed a similar spectral change to that of **Ic**. From the inset shown in Fig. 2, the polyamide **Ic** film switches from a transmissive neutral state (colorless; Y: 85; *x*, 0.313; *y*, 0.330) to a highly absorbing semi-oxidized state (green; Y: 26; *x*, 0.352; *y*, 0.472) and a fully oxidized state (deep purple; Y; 7; *x*, 0.345; *y*, 0.317). The film colorations are distributed homogeneously across the polymer film and survive for more than hundreds of redox cycles. The polymer **Ic** shows a good contrast both in the visible and NIR regions with an extremely high optical transmittance change ($\Delta\%T$) of 54% at 405 nm and 60% at 970 nm for green coloring at the first oxidation stage, and 81% at 865 nm for purple coloring at the second oxidation stage, respectively.

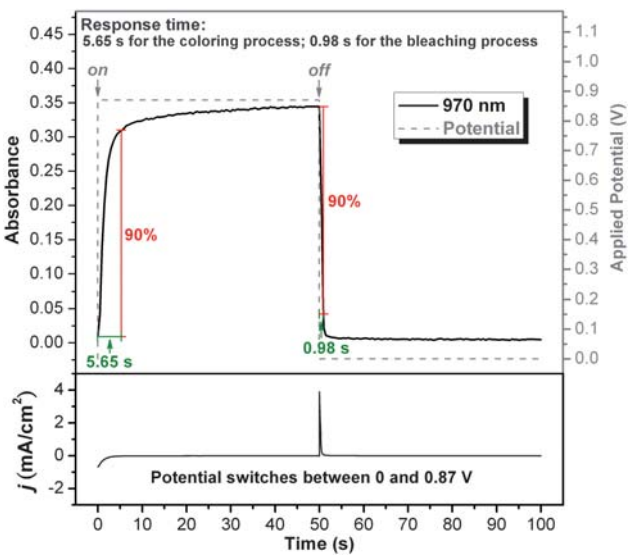

Fig. 4 Calculation of optical switching time at (a) 970 nm and (b) current–time curves of polyamide **Ic** thin film (~70 nm in thickness) on the ITO-coated glass substrate (coated area: 1.2 cm × 0.5 cm) in 0.1 M TBAP/CH_3CN.

Electrochromic switching

For electrochromic switching studies, polymer films were cast on ITO-coated glass slides in the same manner as described above, and chronoamperometric and absorbance measurements were performed. While the films were switched, the absorbance at the given wavelength was monitored as a function of time with UV-vis-NIR spectroscopy. The switching time of polyamide **Ic** shown in Fig. 4 was calculated at 90% of the full switch because it is difficult to perceive any further color change with the naked eye beyond this point. As depicted in Fig. 4(a), polyamide **Ic** thin film revealed a switching time of 5.65 s at 0.87 V for the coloring process at 970 nm and 0.98 s for bleaching. The amounts of Q were calculated by integration of the current density and time obtained from Fig. 4(b) as 1.718 mC cm^{-2} and 1.632 mC cm^{-2} for the oxidation and reduction processes at the first oxidation stage, respectively. The ratio of the charge density was 95.0%, indicating that charge injection/extraction was reversible during the electrochemical reactions. The electrochromic stability of the polyamide **Ic** film was determined by measuring the optical change as a function of the number of switching cycles shown in

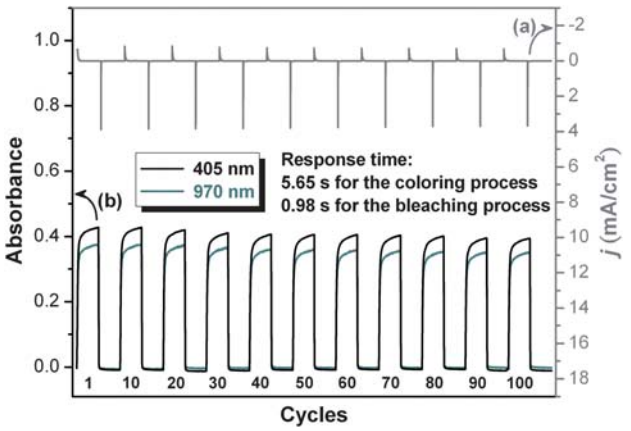

Fig. 5 (a) Current consumption and (b) electrochromic switching between 0 and 0.87 V (*vs.* Ag/AgCl) and absorbance change monitored at 405 nm and 970 nm of polyamide **Ic** thin film (~70 nm in thickness) on the ITO-coated glass substrate (coated area: 1.2 cm × 0.5 cm) in 0.1 M TBAP/CH_3CN with a cycle time of 100 s.

Table 2 Optical and electrochemical data collected for coloration efficiency measurements of polyamide **Ic**

Cycles[a]	δOD_{950}[b]	Q/mC cm^{-2}[c]	η/cm^2 C^{-1}[d]	Decay (%)[e]
1	0.436	1.718	254	0
10	0.434	1.712	254	0
20	0.431	1.704	253	0.4
30	0.423	1.700	249	2.0
40	0.418	1.698	246	3.1
50	0.416	1.693	246	3.1
60	0.414	1.688	245	3.5
70	0.411	1.683	244	3.9
80	0.409	1.676	244	3.9
90	0.401	1.675	239	5.9
100	0.399	1.669	239	5.9

[a] Switching between 0 and 0.95 (V *vs.* Ag/AgCl). [b] Optical density change at 950 nm. [c] Ejected charge, determined from the *in situ* experiments. [d] Coloration efficiency is derived from the equation: $\eta = \delta OD_{950}/Q$. [e] Decay of coloration efficiency after cyclic scans.

Fig. 5. The electrochromic CE ($\eta = \delta OD/Q$) and injected charge (electroactivity) after various switching steps are summarized in Table 2. The electrochromic behavior of **Ic** film exhibited high CE up to 254 cm^2 C^{-1} (at 970 nm) and 390 cm^2 C^{-1} (at 865 nm) at the first and second oxidation stages, respectively, and retained 95% of their electroactivity after hundreds of switching cycles.

Conclusion

A series of NIR electroactive polyamides have been readily prepared from the newly synthesized diamine monomer, 4,4′-diamino-4″-*N*-phenothiazinyltriphenylamine, and various dicarboxylic acids *via* the phosphorylation polyamidation reaction. Introduction of the electron-donating PSN group to the polymer main chain not only affords high T_g and good thermal stability but also leads to good solubility of the polyamides. All the obtained polymers reveal valuable electrochromic characteristics such as enhanced contrast in the NIR region, unique purple electrochromic behavior, low switching times, good coloration efficiency, and high-level electrochromic/electroactive reversibility. Thus, these characteristics indicate the incorporation of pendent PSN groups is a new approach for tuning the coloration change and the prepared polyamides have great potential for applications in both the NIR and visible regions.

Experimental

Materials

N-phenylphenothiazine[16] (**M1**), and 4,4′-Bis(4-benzoylamino)-triphenylamine[12d] (**M2**), were synthesized according to previously reported procedures. Commercially available dicarboxylic acids such as *trans*-1,4-cyclohexanedicarboxylic acid (**5a**), terephthalic acid (**5b**), 4,4′-oxydibenzoic acid (**5c**), and 2,2′-bis(4-carboxyphenyl)hexafluoropropane (**5d**) were purchased from TCI and used as received. Commercially obtained anhydrous calcium chloride ($CaCl_2$) was dried under vacuum at 180 °C for 8 h. Tetrabutylammonium perchlorate (TBAP) (Acros) was recrystallized twice by ethyl acetate under a nitrogen atmosphere and then dried *in vacuo* prior to use. All other reagents were used as received from commercial sources.

Polymer synthesis

The synthesis of polyamide **Ib** was used as an example to illustrate the general synthetic route used to produce a series of polymers. A mixture of 0.24 g (0.5 mmol) of diamine, 4,4′-diamino-4″-*N*-phenothiazinyltriphenylamine (**4**), 0.08 g (0.5 mmol) of terephthalic acid (**5b**), 0.07 g of calcium chloride, 0.5 mL of triphenyl phosphite (TPP), 0.25 mL of pyridine, and 0.5 mL of *N*-methyl-2-pyrrolidinone (NMP) was heated with stirring at 105 °C for 3 h. The obtained polymer solution was poured slowly into 300 mL of stirred methanol giving rise to a stringy, fiberlike precipitate that was collected by filtration, washed thoroughly with hot water and methanol, and dried under vacuum at 100 °C. Reprecipitations of the polymer by DMAc/methanol were carried out twice for further purification. The inherent viscosity and weight-average molecular weights (M_w) of the obtained poly(amine-amide) **Ib** was 0.29 dL/g (measured at a concentration of 0.5 g/dL in DMAc at 30 °C) and 38500, respectively. ^{1}H NMR (DMSO-d_6, δ, ppm): 6.30 (d, 2H, H_c), 6.83 (t, 2H, H_e), 6.96 (t, 2H, H_d), 7.03 (d, 2H, H_f), 7.13 (d, 2H, H_a), 7.21–7.27 (m, 6H, H_b + H_h), 7.83 (d, 4H, H_g), 8.10 (s, 4H, H_i), 10.46 (amide-NH). ^{13}C NMR (DMSO-d_6, δ, ppm): 116.1 (C^6), 119.2 (C^{10}), 122.2 (C^{12} + C^2), 122.8 (C^8), 125.8 (C^{13}), 126.8 (C^9), 127.5 (C^7), 127.9 (C^{16}), 131.6 (C^3), 132.8 (C^4), 135.5 (C^{14}), 137.7 (C^{15}), 142.7 (C^5), 144.2

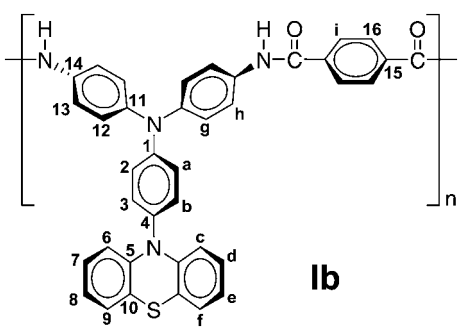

(C^{11}), 147.6 (C^{1}), 164.9 (amide carbonyl). The other polyamides were prepared by an analogous procedure.

Preparation of the polyamide films

A solution of polymer was made by dissolving about 0.3 g of the polyamide samples in 8 mL of DMAc or NMP. The homogeneous solution was poured into a 9-cm glass Petri dish, which was placed in a 80 °C oven for 6 h to remove most of the solvent; then the semidried film was further dried *in vacuo* at 180 °C for 8 h. The obtained films were about 30–50 μm in thickness and were used for molecular weight measurements, solubility tests, and thermal analyses.

Measurements

Fourier transform infrared (FT-IR) spectra were recorded on a Perkin Elmer RXI FT-IR spectrometer. Elemental analyses were run in a VarioEL-III Elementar. Fast atom bombardment (FAB) mass spectra were measured on JEOL MStation JMS-700 mass spectrometer. ^{1}H and ^{13}C nuclear magnetic resonance (NMR) spectra were measured on a Bruker AV-300 FT-NMR system and referenced to the DMSO-d_6 signal, and peak multiplicity was reported as follows: s, singlet; d, doublet; t, triplet; m, multiplet. The inherent viscosities were determined at 0.5 g/dL concentration using a Tamson TV-2000 viscometer at 30 °C. Gel permeation chromatographic (GPC) analysis was performed on a Lab Alliance RI2000 instrument (one column, MIXED-D from Polymer Laboratories) connected with a refractive index detector from Schambeck SFD Gmbh. All GPC analyses were performed using a polymer/DMF solution at a flow rate of 1 mL min^{-1} at 70 °C and calibrated with polystyrene standards. Thermogravimetric analysis (TGA) was conducted with a Perkin Elmer Pyris 1 TGA. Experiments were carried out on approximately 6–8 mg film samples heated in flowing nitrogen or air (flow rate: 20 cm^3 min^{-1}) at a heating rate of 20 °C min^{-1}. DSC analyses were performed on a Perkin Elmer Pyris Diamond DSC at a scan rate of 20 °C min^{-1} in flowing nitrogen (flow rate: 20 cm^3 min^{-1}). Thermomechanical analysis (TMA) was conducted with a Perkin Elmer Diamond TMA instrument. The TMA experiments were conducted from 50 to 350 °C at a scan rate of 10 °C min^{-1} with a penetration probe 1.0 mm in diameter under an applied constant load of 50 mN. Softening temperatures (T_s) were taken as the onset temperatures of probe displacement on the TMA traces. Ultraviolet-visible (UV-vis) spectra of the polymer films were recorded on a Varian Cary 50 Probe spectrometer. Absorption spectra in spectroelectochemical analysis were measured with a HP 8453 UV-Visible spectrophotometer. All spectra were obtained by averaging five scans. Cyclic voltammetry (CV) was conducted with the use of a three-electrode cell in which ITO (polymer films area about 0.5 cm × 1.2 cm) was used as a working electrode. A platinum wire was used as an auxiliary electrode. All cell potentials were taken by using a homemade Ag/AgCl, KCl (sat.) reference electrode in dry acetonitrile (CH_3CN) and *N*,*N*-dimethylformamide (DMF) solution of 0.1 M tetrabutylammonium perchlorate (TBAP) under a nitrogen atmosphere for oxidation and reduction measurements, respectively. Spectroelectrochemical experiments were carried out in a cell built from a 1 cm commercial UV-visible cuvette using a Hewlett-Packard 8453 UV-Visible diode array spectrophotometer. The ITO-coated glass slide was used as the working electrode, a platinum wire as the counter electrode, and a Ag/AgCl cell as the reference electrode. CE (η) determines the amount of optical density change (δOD) at a specific absorption wavelength induced as a function of the injected/ejected charge (Q; also termed as electroactivity) which is determined from the *in situ* experiments. CE is given by the equation: $\eta = \delta OD/Q = \log[T_b/T_c]/Q$, where η (cm^2 C^{-1}) is the coloration efficiency at a given wavelength, and T_b and T_c are the bleached and colored transmittance values, respectively. The thickness of the polyamide thin films was measured by an alpha-step profilometer (Kosaka Lab., Surfcorder ET3000, Japan). Colorimetry measurements were obtained using a Minolta CS-100A Chroma Meter. The color coordinates are expressed in the CIE 1931 Yxy color spaces.

Acknowledgements

The authors are grateful to the National Science Council of the Republic of China for financial support of this work. The technical assistance on the gel permeation chromatographic measurement from Prof. Wen-Chang Chen and Dr Chia-Hung Lin of National Taiwan University is highly appreciated.

References and notes

1 (*a*) P. M. S. Monk, R. J. Mortimer and D. R. Rosseinsky, *Electrochromism: Fundamentals and Applications*; VCH: Weinheim, Germany, 1995; (*b*) R. J. Mortimer, *Chem. Soc. Rev.*, 1997, **26**, 147; (*c*) D. R. Rosseinsky and R. J. Mortimer, *Adv. Mater.*, 2001, **13**, 783; (*d*) P. R. Somani and S. Radhakrishnan, *Mater. Chem. Phys.*, 2003, **77**, 117; (*e*) S. Liu, D. G. Kurth, H. Mohwald and D. Volkmer, *Adv. Mater.*, 2002, **14**, 225; (*f*) T. Zhang, S. Liu, D. G. Kurth and C. F. J. Faul, *Adv. Funct. Mater.*, 2009, **19**, 642; (*g*) A. Maier, A. R. Rabindranath and B. Tieke, *Adv. Mater.*, 2009, **21**, 959; (*h*) L. Motiei, M. Lahav, D. Freeman and M. E. van der Boom, *J. Am. Chem. Soc.*, 2009, **131**, 3468; (*i*) P. M. Beaujuge and J. R. Reynolds, *Chem. Rev.*, 2010, **110**, 268.

2 (*a*) U. Bach, D. Corr, D. Lupo, F. Pichot and M. Ryan, *Adv. Mater.*, 2002, **14**, 845; (*b*) A. L. Dyer, C. R. G. Grenier and J. R. Reynolds, *Adv. Funct. Mater.*, 2007, **17**, 1480; (*c*) C. Ma, M. Taya and C. Xu, *Polym. Eng. Sci.*, 2008, **48**, 2224; (*d*) S. Beaupre, A. C. Breton, J. Dumas and M. Leclerc, *Chem. Mater.*, 2009, **21**, 1504.

3 (*a*) T. L. Rose, S. D'Antonio, M. H. Jillson, A. B. Kon, R. Suresh and F. Wang, *Synth. Met.*, 1997, **85**, 1439; (*b*) E. B. Franke, C. L. Trimble, J. S. Hale, M. Schubert and J. A. Woollam, *J. Appl. Phys.*, 2000, **88**, 5777; (*c*) P. Topart and P. Hourquebie, *Thin Solid Films*, 1999, **352**, 243; (*d*) P. Chandrasekhar, B. J. Zay, T. McQueeney, A. Scara, D. Ross, G. C. Birur, S. Haapanen, L. Kauder, T. Swanson and D. Douglas, *Synth. Met.*, 2003, **135–136**, 23.

4 (*a*) S. J. Vickers and M. D. Ward, *Electrochem. Commun.*, 2005, **7**, 389; (*b*) P. F. H. Schwab, S. Diegoli, M. Biancardo and C. A. Bignozzi, *Inorg. Chem.*, 2003, **42**, 6613; (*c*) Y. Qi and Z. Y. Wang, *Macromolecules*, 2003, **36**, 3146; (*d*) S. Wang, E. K. Todd, M. Birau, J. Zhang, X. Wan and Z. Y. Wang, *Chem. Mater.*, 2005, **17**, 6388; (*e*) W. Qiao, J. Zheng, Y. Wang, Y. Zheng, N. Song, X. Wan and Z. Y. Wang, *Org. Lett.*, 2008, **10**, 641; (*f*) J. Zheng, W. Qiao, X. Wan, J. P. Gao and Z. Y. Wang, *Chem. Mater.*, 2008, **20**, 6163; (*g*) F. Hasanain and Z. Y. Wang, *Dyes Pigm.*, 2009, **83**, 95.

5 (*a*) B. Sankaran and J. R. Reynolds, *Macromolecules*, 1997, **30**, 2582; (*b*) G. Sonmez, H. Meng, Q. Zhang and F. Wudl, *Adv. Funct. Mater.*, 2003, **13**, 726; (*c*) G. Sonmez, H. Meng and F. Wudl, *Chem. Mater.*, 2004, **16**, 574; (*d*) M. Li, A. Patra, Y. Sheynin and M. Bendikov, *Adv. Mater.*, 2009, **21**, 1707.

6 (*a*) A. Higuchi, H. Inada, T. Kobata and Y. Shiraota, *Adv. Mater.*, 1991, **3**, 549; (*b*) S. A. Jenekhe, L. Lu and M. M. Alam,

Macromolecules, 2001, **34**, 7315; (*c*) W. Wu, J. Yang, J. Hua, J. Tang, L. Zhang, Y. Long and H. Tian, *J. Mater. Chem.*, 2010, **20**, 1772.
7 (*a*) R. Y. Lai, X. Kong, S. A. Jenekhe and A. J. Bard, *J. Am. Chem. Soc.*, 2003, **125**, 12631; (*b*) X. Kong, A. P. Kulkarni and S. A. Jenekhe, *Macromolecules*, 2003, **36**, 8992; (*c*) M. J. Park, J. Lee, J. H. Park, S. K. Lee, J. I. Lee, H. Y. Chu, D. H. Hwang and H. K. Shim, *Macromolecules*, 2008, **41**, 3063; (*d*) N. S. Cho, J. H. Park, S. K. Lee, J. Lee, H. K. Shim, M. J. Park, D. H. Hwang and B. J. Jung, *Macromolecules*, 2006, **39**, 177.
8 D. Sun, S. V. Rosokha and J. K. Kochi, *J. Am. Chem. Soc.*, 2004, **126**, 1388.
9 (*a*) M. Thelakkat, *Macromol. Mater. Eng.*, 2002, **287**, 442; (*b*) Y. Shirota, *J. Mater. Chem.*, 2005, **15**, 75; (*c*) Y. Shirota and H. Kageyama, *Chem. Rev.*, 2007, **107**, 953; (*d*) T. Kuorosawa, C. C. Chueh, C. L. Liu, T. Higashihara, M. Ueda and W. C. Chen, *Macromolecules*, 2010, **43**, 1236.
10 (*a*) Y. Oishi, M. Ishida, M. A. Kakimoto, Y. Imai and T. Kurosaki, *J. Polym. Sci., Part A: Polym. Chem.*, 1992, **30**, 1027; (*b*) G. S. Liou, S. H. Hsiao, M. Ishida, M. A. Kakimoto and Y. Imai, *J. Polym. Sci., Part A: Polym. Chem.*, 2002, **40**, 3815; (*c*) M. K. Leung, M. Y. Chou, Y. O. Su, C. L. Chiang, H. L. Chen, C. F. Yang, C. C. Yang, C. C. Lin and H. T. Chen, *Org. Lett.*, 2003, **5**, 839; (*d*) M. Y. Chou, M. K. Leung, Y. O. Su, C. L. Chiang, C. C. Lin, J. H. Liu, C. K. Kuo and C. Y. Mou, *Chem. Mater.*, 2004, **16**, 654; (*e*) L. Otero, L. Sereno, F. Fungo, Y. L. Liao, C. Y. Lin and K. T. Wong, *Chem. Mater.*, 2006, **18**, 3495.
11 (*a*) S. H. Cheng, S. H. Hsiao, T. H. Su and G. S. Liou, *Macromolecules*, 2005, **38**, 307; (*b*) T. H. Su, S. H. Hsiao and G. S. Liou, *J. Polym. Sci., Part A: Polym. Chem.*, 2005, **43**, 2085.
12 (*a*) C. W. Chang, G. S. Liou and S. H. Hsiao, *J. Mater. Chem.*, 2007, **17**, 1007; (*b*) G. S. Liou and C. W. Chang, *Macromolecules*, 2008, **41**, 1667; (*c*) S. H. Hsiao, G. S. Liou, Y. C. Kung and H. J. Yen, *Macromolecules*, 2008, **41**, 2800; (*d*) C. W. Chang, C. H. Chung and G. S. Liou, *Macromolecules*, 2008, **41**, 8441; (*e*) C. W. Chang and G. S. Liou, *J. Mater. Chem.*, 2008, **18**, 5638; (*f*) C. W. Chang, H. J. Yen, K. Y. Huang, J. M. Yeh and G. S. Liou, *J. Polym. Sci., Part A: Polym. Chem.*, 2008, **46**, 7937; (*g*) H. J. Yen and G. S. Liou, *Chem. Mater.*, 2009, **21**, 4062; (*h*) S. H. Hsiao, G. S. Liou and H. M. Wang, *J. Polym. Sci., Part A: Polym. Chem.*, 2009, **47**, 2330.
13 J. M. Garcia, F. C. Garcia, F. Serna and J. L. de la Pena, *Prog. Polym. Sci.*, 2010, **35**, 623.
14 (*a*) N. Yamazaki, F. Higashi and J. Kawabata, *J. Polym. Sci., Polym. Chem. Ed.*, 1974, **12**, 2149; (*b*) N. Yamazaki, M. Matsumoto and F. Higashi, *J. Polym. Sci., Polym. Chem. Ed.*, 1975, **13**, 1373.
15 G. Gritzner and J. Kutta, *Pure Appl. Chem.*, 1984, **56**, 461.
16 H. Gilman, P. R. Van Ess and D. A. Shirley, *J. Am. Chem. Soc.*, 1944, **66**, 1214.

